

MAGNETIC FIELD DISTRIBUTION DETECTING AND COMPUTING METHODS FOR EXPERIMENTAL MECHANICS

J. Kaleta, P. Wiewiórski

Wroclaw University of Technology
Institute of Materials Science and Applied Mechanics

Smoluchowskiego 25, 50-370 Wroclaw, Poland
e-mail: {jerzy.kaleta, przemyslaw.wiewiorski}@pwr.wroc.pl

This paper presents the design and measuring potential of the latest generation of the magnetic scanner called Magscanner-Maglab System (MMS) which enables a fast acquisition of 3D signals from magnetic sensors and their visualization as digitalized magnetic images for a variety of flat and cylindrical objects. MMS can be used as entirely autonomous or combined (through common control) with a typical material testing machine for static load and fatigue tests. The system can be used to investigate magnetomechanical phenomena and identify their models in experimental mechanics, as well as detect and locate strain fields, areas of plastic deformations and cracks in industrial processes. It has been used recently to measure the magnetic field around objects subjected to technological processing in order to check their quality.

1. INTRODUCTION AND RESEARCH OBJECTIVE

Digital visualization is used by various systems (based on discrete sensors or a matrix of sensors) for the human optical perception of real physical effects. Optoelectronic CCD digital cameras or thermal infrared imaging cameras are commonly employed for this purpose. In recent years attempts have been made to visualize the magnetic field by magnetovision cameras. A new NDT/NDE method, called magnetovision, based on such cameras has been developed. The method has found a number of applications in the technology and medicine [1–3]. All ferromagnetic materials can be investigated in this way. The most promising application areas for magnetovision are inverted magnetostriction (also referred to as the Villari effect¹⁾) and examination of Smart Magnetic Materials (SMM) [4]. The current research and engineering aim of such experiments is to identify physical models of the Villari effect, which could be used to determine the strain field on the basis of magnetic field strength vector components.

¹⁾Villari Effect – the effect of mechanical deformation (stretching, twisting, and bending) on the magnetization of a ferromagnetic. Discovered in 1865 by the Italian physicist E. Villari (1836–1904), the effect is the opposite of magnetostriction, i.e., change in the size of a ferromagnetic during magnetization.

The authors' earlier papers presented the foundations of the new diagnostic technique and the possibilities of developing a magnetovision apparatus. They also described the metrological properties of the Villari effect [1, 5, 6] and discussed the possibilities of applying magnetovision in fatigue tests, crack tests [7], and texture tests [8, 9], as well as in athermal martensitic transformations [10, 11].

The development of magnetovision has several limitations whereby it has not been as spectacular as that of thermovision or optoelectronic CCD techniques. The visualization of a scalar quantity, such as temperature, is easy to interpret, whereas the representation of a vector quantity, such as magnetic field strength, in the form of 2D or 3D maps, taking into account the investigated object's geometry, is a much more difficult task. Another difficulty lies in the fact that at the moment no magnetic field sensors in the form of matrices (such as CCD sensor matrices) are available.

Considering the above, a method of measuring the 3D magnetic field in experimental mechanics was chosen as the main objective of this research. In order to achieve the objective the following key tasks were planned:

- developing a non-contact magnetic field strength measurement concept;
- constructing an apparatus (scanner) for investigation of, in particular, flat and cylindrical objects;
- creating a software for measuring, processing and visualization of the magnetic field;
- making identification of magnetomechanical cross effects (the Villari effect) possible;
- providing examples of application of the magnetic field measuring method in investigation of the state of mechanical and SMM objects.

The mentioned above tasks are discussed successively below.

2. IDEA OF A NON-CONTACT MEASUREMENT OF THE MAGNETIC FIELD

It was assumed that a magnetic field strength should be measured without any contact with the investigated object. Also, the measurement method should allow one to determine the values of the magnetic field components, respectively H_x , H_y , H_z , at different distances d from the investigated object, starting from very small distances (as small as 0.10 mm). This is vital since as distance d increases details are lost in the leakage flux above the object. By scanning the plane located at d_{\min} and performing scans of successive planes distant by Δd from each other, one can determine the magnetic leakage flux over the investigated object and also along the perpendicular axis (Z). The idea of the measurement is illustrated in Fig. 1.

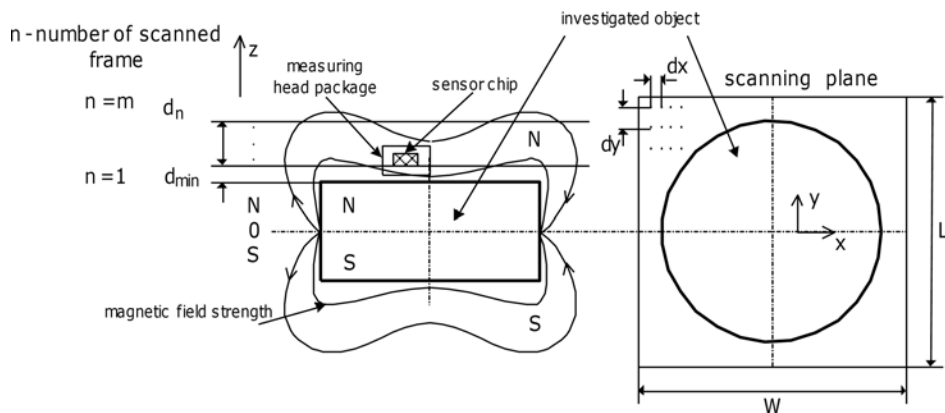


FIG. 1. Scanning with the measuring head with passive sensors to determine the magnetic field strength distribution around the investigated object.

The results of scanning with passive sensors of the plane located at distance d from the investigated object need to be properly interpreted. In this measurement technique each magnetic field strength reading contains information about the entire geometry of the investigated object. Figure 2 schematically shows the location of the measuring head in space and how its position is ascertained by means of radii R_i and appropriate angles ϕ_i . Consequently, the two-dimensional map obtained for a given magnetic field vector component is the result of the stereographic projection of the investigated object onto the scanning plane.

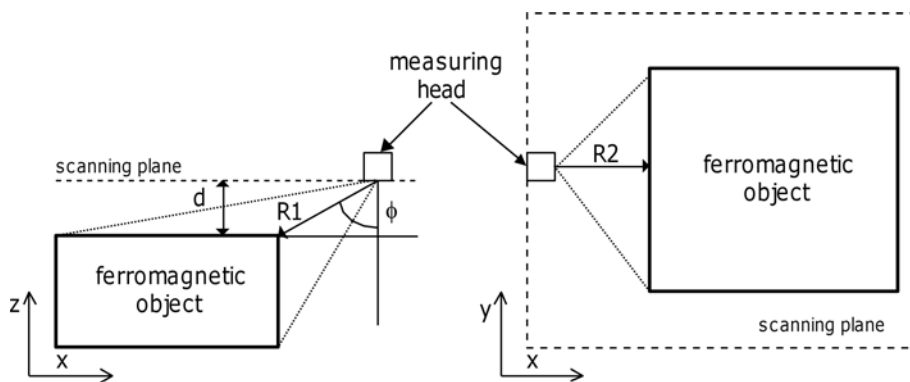


FIG. 2. Scanning of the plane above the investigated object. Interpretation of a 2D map for a given magnetic field vector component, as a stereographic projection of the investigated object onto the scanning plane.

In order to fully investigate the magnetomechanical phenomenon one needs various magnetic field sensors. Passive magnetic field sensors (mainly magnetoresistance sensors and Hall sensors) have been chosen in order to ensure that the magnetic field strength around the investigated object remains undisturbed.

Due to advanced passive magnetic field sensors now all the three components of the magnetic field strength vector can be measured in a single geometric point in space. Since there is a wide range of sensors available, measurements in a wide range of magnetic strength values become possible. The types of sensors used for the particular subranges are:

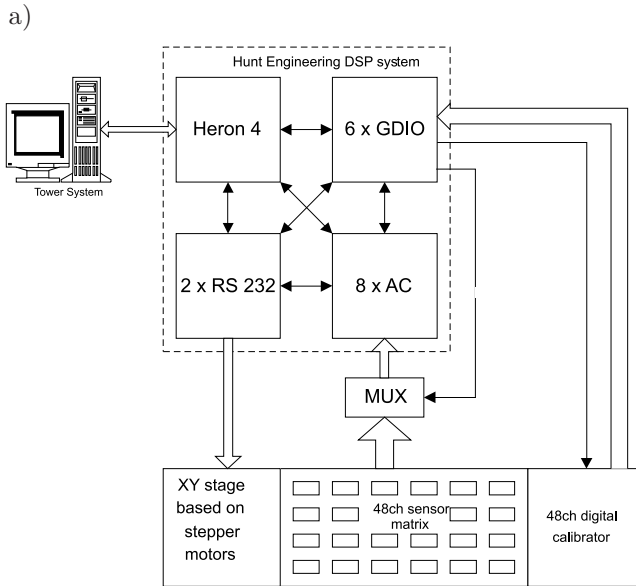
- weak magnetic fields ($0.1\text{--}100\ \mu\text{T}$) – anisotropic magnetoresistance (AMR) sensors;
- medium magnetic fields ($50\ \mu\text{T} - 10\ \text{mT}$) – giant magnetoresistance (GMR) sensors;
- high magnetic fields ($10\ \text{mT}$ up to $2000\ \text{mT}$) – Hall elements.

Availability of advanced thin-film magnetic field sensors and the introduction of motion processors incorporating a real time operation system (RTOS) have made a 3D visualization of the magnetic field vector by a third generation scanner (magnetovision camera) possible. The scanner features a range of state-of-the-art sensors, software, and mechanical structures. For over a decade the team to which the present authors belong has developed several generations of cameras and scanners which can take magnetic images of materials subjected to various kinds of treatment, mechanic loads, and phase transformations.

3. MULTISENSOR MAGNETIC FIELD MEASURING SYSTEM

In the literature one can find solutions which can be used to quickly determine a magnetic field distribution by means of a considerable number of sensors (with identical parameters and characteristics) arranged on a scanning plane [12]. An earlier version of the multisensor magnetovision system recorded magnetic field strength by means of its 60×40 mm flat measuring head. The solution was based on a system with a digital signal processor (DSP). The measuring unit consisted of a matrix of 48 Philips KMZ52 magnetoresistance sensors. It incorporated analogue and digital circuits shaping the signal and reducing noise as well as ensuring proper data transmission to the signal processing unit. The DSP card, capable of fast data processing and having a large number of input/output interfaces, generated magnetic field maps in real time for two magnetic field components in 24 points. In order to obtain higher resolution maps it was necessary to use an XY positioner and scanning mode operation.

Figure 3 shows the structure of the magnetovision system. A Hunt Engineering HERON card incorporating a C6701 digital signal processor forms its signal processing unit. Conversion of measurement data into the digital form and their final processing is the task of this part of the measuring system. Signal processing is understood here as digital processing of signals, i.e., decoding, digital filtration, and Fourier transformation.



b)

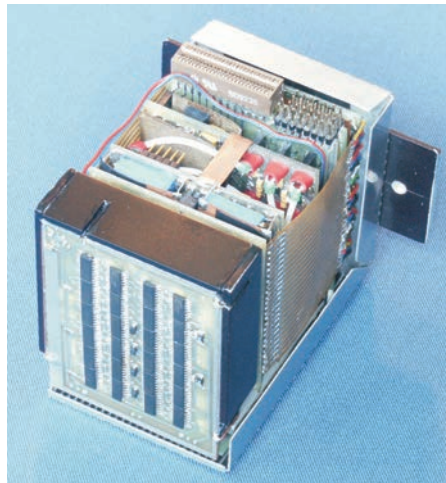
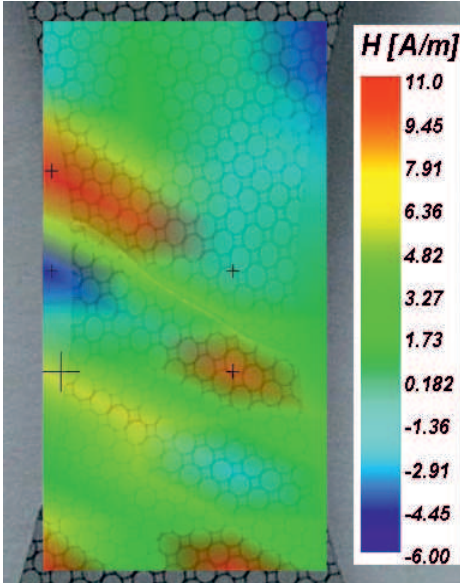


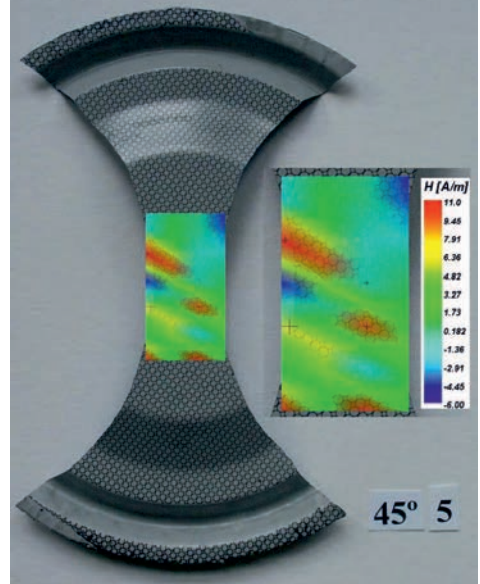
FIG. 3. Multisensor magnetovision system: a) system structure, b) measuring head with 48 magnetic field sensors.

The above system was used mainly to monitor metal sheet forming and to determine the formability of metal sheets and the texture of the material [8, 9]. Figure 4 shows exemplary results of monitoring the metal sheet forming process and determining the loss of stability by the metal sheet. The experience gained in the building of the system was then used to create magnetic field scanning devices based on 3D sensors.

a)



b)



c)

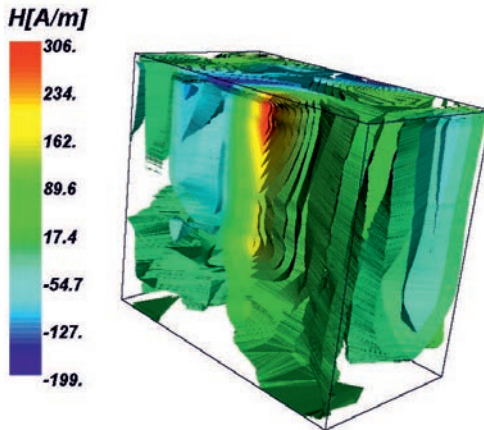


FIG. 4. Exemplary results of monitoring a metal sheet forming process and determining the loss of stability by a metal sheet: a) magnetic field map superimposed on the crack area, b) die stamping with a crack, c) isosurfaces of the magnetic field variation during the forming.

4. MAGNETIC FIELD SCANNER AND THE INVESTIGATION METHODOLOGY

The main components of the magnetic field scanner and its software, as well as exemplary applications of the measuring system in experimental mechanics, are presented below.

4.1. Scanner design

The main objectives achieved in the Magscanner system project are:

- a mobile modular measuring system;
- a wide programmable range of mechanical movements of the movable part incorporating a measuring head;
- scanning parameters, i.e., the set position and scanning speed, controlled by a motion processor based on RTOS;
- the measuring head (an autonomous part of the system) is a complete analogue measuring circuit which can be replaced with another one with different specifications;
- all scanning operations are controlled by a single dedicated software.

A block diagram of the Magscanner system is shown in Fig. 5. The control unit of Magscanner consists of the following components (Fig. 5a):

- an IBM T30 computer with a docking station using a PCI control card to serve all Magscanner operations;
- an advanced motion control system APCI-8001 by ADDI-DATA. The motion controller incorporated in the APCI-8001 controls scanner precision positioning and ensures its optimal dynamics;
- a sensor signal acquisition system based on DT9804 by Data Translation, with a digital trigger to synchronize carriage positions and analogue values from the sensors;
- software dedicated to Magscanner/Maglab, controlling the whole system and visualizing the results. A lot of effort has been put into the development of this software. Recently the part responsible for further processing of the results has been separated from Magscanner and called Maglab. This software package enables export of the results to CAD systems and visualization of the magnetic field vector in a 3D space.

The Magscanner system has been adapted to perform several tasks in the field of experimental mechanics. Now this magnetovision system has four independent magnetic inspection subsystems (shown in Fig. 5b):

- an advanced XYZ scanner which can work in tandem with material testing machines (MTS). The guaranteed resolution of the measuring head travel is 2160 DPI. In terms of functionality, the measuring head's positioning system is based on the same principle as the professional A3+ format scanners, e.g., the AGFA DuoScan series. The working scanning range is $410 \times 180 \times 200$ mm. The Z axis enables performance of a series of scans for a set distance from the investigated object, and it is also needed to install the system on a strength testing machine in order to

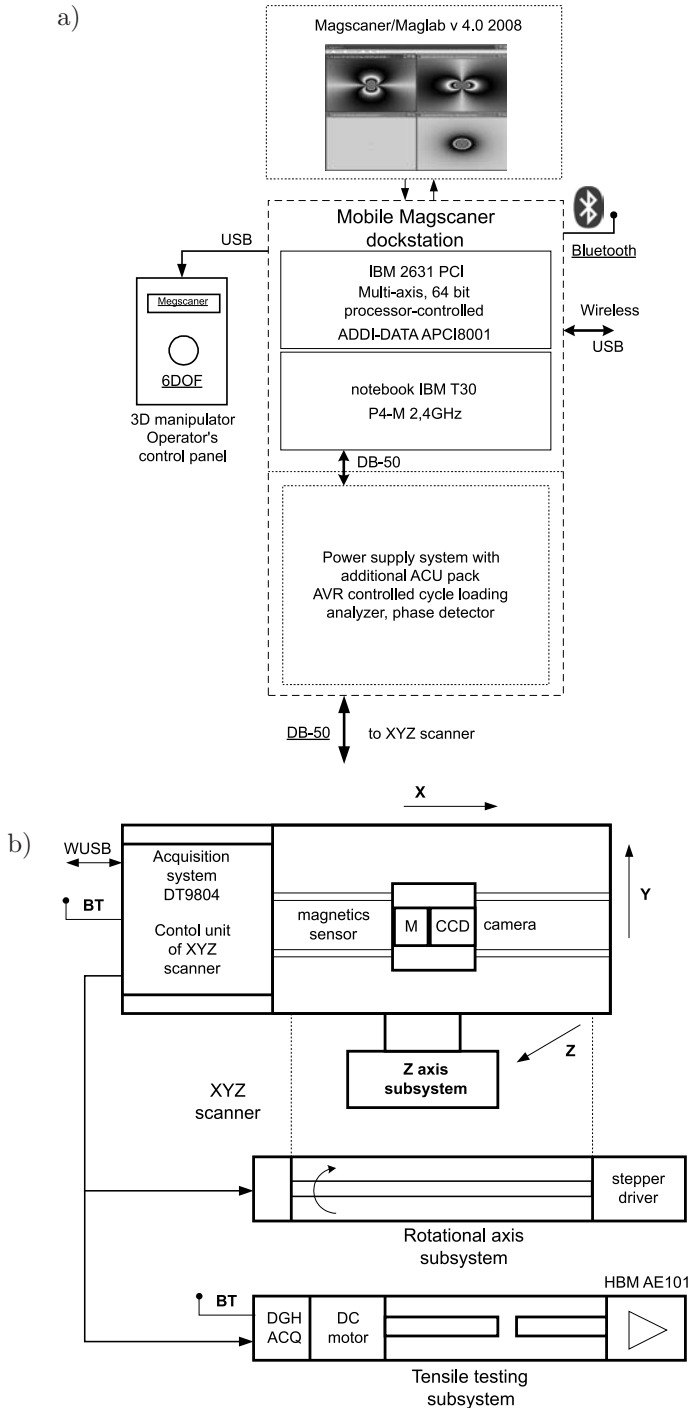


FIG. 5. Block diagram of the magnetic field scanner: a) computer-aided system, b) subsystems: XYZ scanner, rotational scanner, tensile testing machine.

acquire maps of magnetic field distribution maps from, e.g. a fatigue process;

- measurement heads based on:
 - Honeywell HMC1053 – for WMF and MMF;
 - Allegro Micro RMT34 Hall elements – for HMF;
- a rotational axis analyzer – a subsystem designed for measuring and analyzing magnetic field distribution around axisymmetrical elements (e.g., cylinders and pipes), mainly with quick industrial tests in mind. The al-

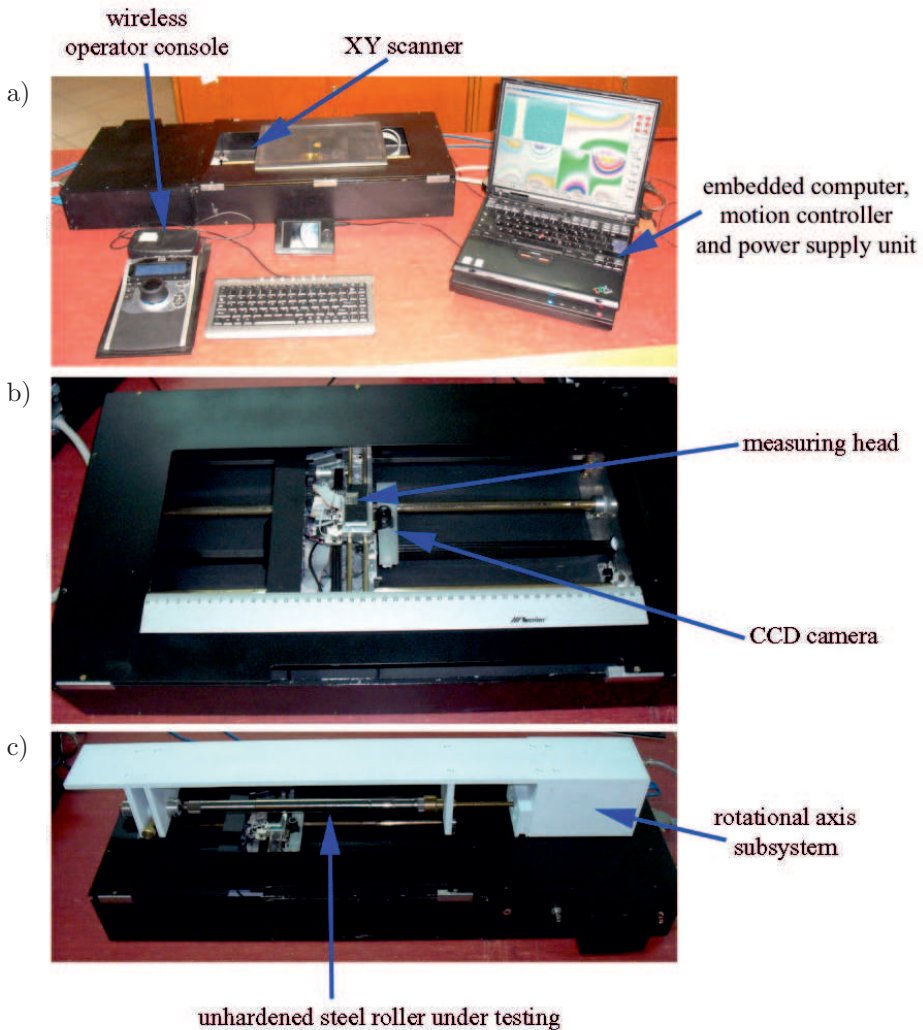


FIG. 6. Magscanner system: a) scanner setup, b) XY scanner, c) scanner for axisymmetrical objects.

gorithm can be used for testing of magnetic and electrostatic cylinders in refabrication of toner cassettes for laser printers. Currently, research on potential applications in the car industry is being conducted;

- a micro-tensile testing machine – a device enabling precise measurements of the magnetic field and mechanical quantities for foil materials subjected to static strength tests. The beam scanning movement resolution is 0.25 micrometers. The force of 1.0–500 N can be measured thanks to an HBM AE101 amplifier (class 0.1%).

All the subsystems are controlled by the same control unit and by the Magscanner software. The magnetovision scanner and its components are shown in Fig. 6.

Figure 6a shows the magnetic scanner setup. One of the major advantages of the system is its mobility. The number of cables has been reduced to an absolute minimum. A wireless operator panel (based on the wireless USB standard) has been introduced. The main scanner functions can be controlled from the panel. Figure 6b shows the measurement zone of the XY scanner including a measuring head and a CCD camera for recording the scanning of the investigated object. In order to illustrate the capabilities of the Magscanner, the way of setting up the subsystem for scanning cylindrical objects is shown in Fig. 6c.

4.2. Scanner measuring specifications

The main specifications of the Magscanner system and its subsystems are as follows:

- range of magnetic field measurement at 16 bit ADC resolution:
 - WMF: a 0.1–100 μT AMR head based on the Philips KMZ5x series MR,
a 1.0–500 μT AMR head based on a modified Honeywell HMC105x series MR;
 - MMF: a 50 μT – 10 mT AMR head based on the Philips KMZ1x series MR,
a 1–100 mT head based on Hall elements by Allegro Micro;
 - MMF/HMF: a 20–2000 mT head based on RMT34 Hall elements by Allegro Micro;
- max. scanning speed – 50 000 points/sec;
- max. scanning resolution – 2160 DPI (0.02 mm);
- max. number of scanned magnetic field points – 20 million points (maps as large as 20000 \times 1000);
- DT 9804 card sampling frequency at 16-bit resolution – 100 kHz.

4.3. Preparation of measuring heads

The measuring heads are decisive for achieving a satisfactory magnetic field measurement quality. There is no universal measuring head which could be used for measurements in the whole magnetic field range. Also, the size and shape of the head depend on the peculiarities of the investigated object and on the number and size of the sensors used. A head for measuring flat surfaces will be different from the one for determining a magnetic field distribution on cylindrical surfaces. In a triaxial head the three magnetic field sensors perpendicular to each other should be located possibly in one point in space. For example, an integrated Hall probe was made by sticking together three Hall sensors (for H_x , H_y and H_z , respectively), each with their own independent conditioning system. Due to the small dimensions of the Hall-effect magnetic field measuring system ($3 \times 3 \times 2 \text{ mm}^3$), quasi-point measurements (necessary in the case of cylindrical surfaces) can be performed. A special head based on Honeywell HMC1053 magnetoresistors was developed for the triaxial measurement of the magnetic field vector on a flat surface. Measurements can also be made using a head based on Philips KMZ52 or KMZ51 magnetoresistors.

4.4. Maglab software – a complete tool for magnetomechanical evaluation

Maglab software is a major component of the Magscanner system. The proposed method of evaluating the magnetic field distribution around different objects is based on modified passive sensors made by Honeywell and on the dedicated Magscanner/Maglab software which is compatible with industrial parametric CAD systems (e.g., ProEngineer and Solid Works) and with NURBS (Rhinoceros). The measurement technique consists in acquiring a set of points belonging to equally distant planes, similarly as in tomography and 3D visualization in CAD under the IGES standard.

The possibilities offered by the Magscanner-Maglab systems are presented below. Two aluminium plates (discs) with circular holes aligned in parallel were the test objects. The plates that were connected to a power source were subjected to a quasistatic tension until rupture. The direction of the current (reverse in both plates) is shown in Fig. 7. Such a process, combining both the mechanical and electrical loadings of the plates, is hard to describe analytically. Visualization of the magnetic field with the use of commercially available systems is difficult or even impossible.

Figure 8 shows Maglab windows with magnetic field strength distribution maps before uniaxial tension and immediately after the failure of a set of two plates with holes. As the plates were under tension, a current of 1 A was flowing through them. Figure 8a shows the image from the photodiode (PD; the geo-

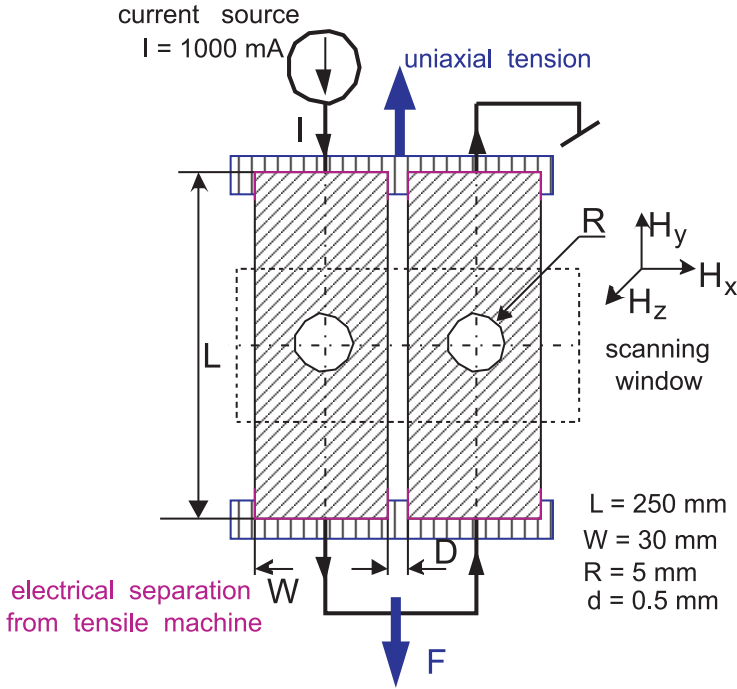


FIG. 7. Scheme of the uniaxial tension of the aluminium plates connected to a power source.

metric resolution is identical to the resolution of the magnetic sensors) and the distribution of the H vector components, marked subsequently as H_y , H_z , H_x . To the right, the courses of these quantities are presented for the cross-section drawn through the middle of the holes. Analogous characteristics for the final phase of the sample rupture are shown in Fig. 8b. Additionally, the embedded colour scheme generator is presented in Fig. 8c.

The main features and modules of the Maglab software are as follows:

- four windows: MagnX, MagnY, MagnZ, showing (with a set resolution) the distribution of the three magnetic field vector components in the scanned area, and the Camera window showing a map received from an optical sensor;
- the possibility of a simultaneous work on 10 different projects stored in the clipboard for comparisons and further analyses;
- high resolution of the maps, dependent on the sensor distance from the investigated object;
- the possibility of displaying multiframe projects a movie;
- a built-in module for creating and selecting the best spectrum of colours (the Pattern of colours in Fig. 8c) to represent the determined distributions;

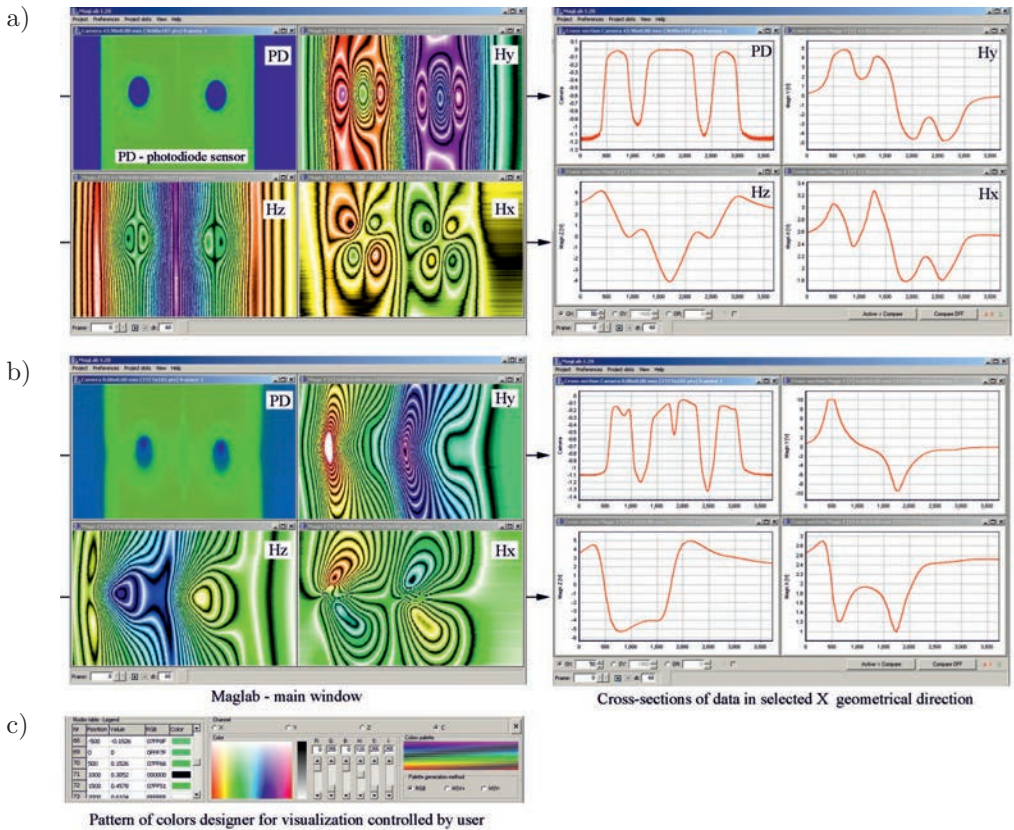


FIG. 8. Features of the Maglab software for the sample subjected to tension and connected to a power source (as shown in Fig. 7).

- a sensor position correction module enabling fitting of the maps that come from the sensors located in different points;
- a Cross sections module enabling the user to create and edit linear cross sections from the acquired maps;
- a Hysteresis module enabling generation of waveforms in specified coordinates and time domain;
- the Magscanner/Maglab software package enables further processing and visualization of the magnetic field distribution maps in a CAD program (ProEngineer) or in NURBS (Rhinceros);
- Maglab allows one to quickly generate maps of the stress distribution, strains, and the specific energy for the Kirsch problem.

In addition, Maglab has basic magnetostatic models implemented as standards for experimental measurements. Strong emphasis has been placed on the way results are presented and on optimization of calculations. Therefore, the

software package can find many applications also in other areas requiring knowledge of magnetic field distribution. In the nearest future, the main application area will be identification of magnetomechanical dependences for a plate with a central hole subjected to fatigue.

Due to visualization of an elementary magnetic field vector distribution as a stereographic projection [13] it was possible to develop the Dipole Contour Method (DCM) which has been implemented in the Magscanner-Maglab software package [14]. The concept of DCM and other related notions shown in Fig. 9. This method is used to visually represent information supplied by data.

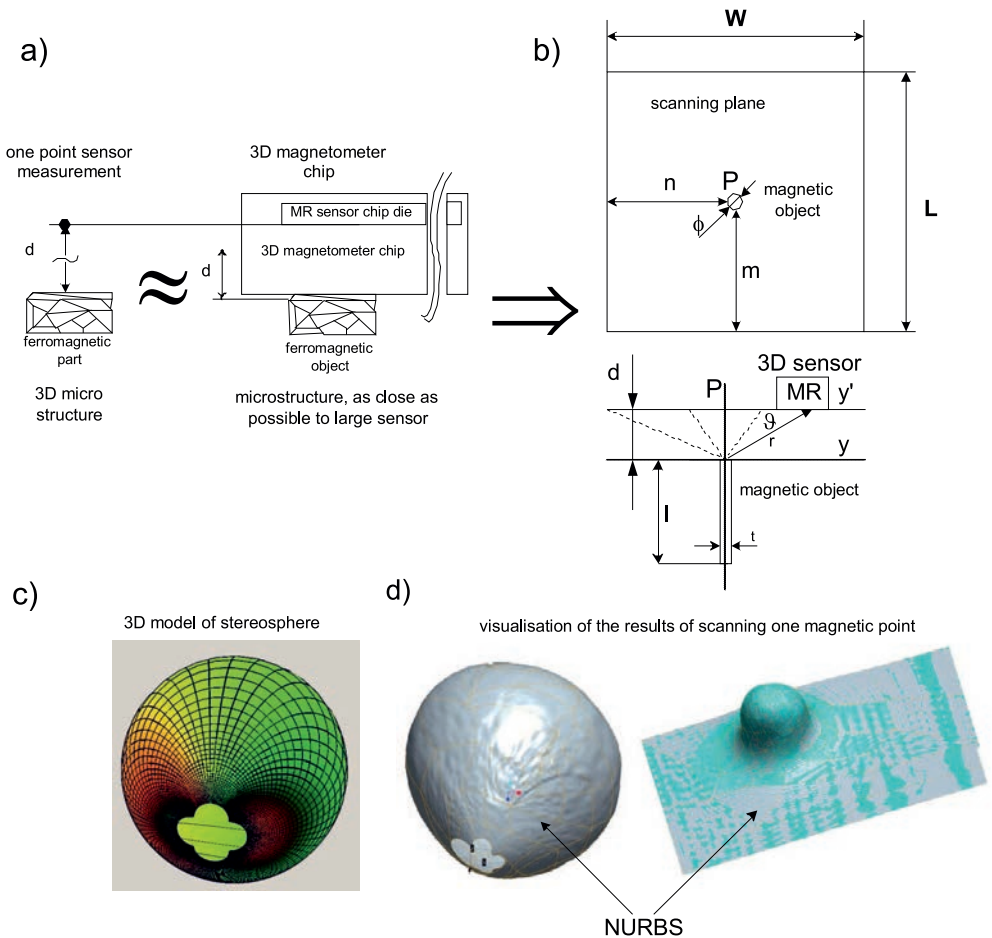


FIG. 9. Magnetic field distribution as a stereographic projection [14]: a) distance d and sensor chip are not small enough to measure elementary micromagnetism, b) single point magnetic object produces stereographic projection, c) stereosphere obtained from the model and from the experiment (d) as a flat area magnetic field distribution. It should be emphasized that the stereosphere from the experiment was created with the use of many NURBS surfaces.

Since due to its size the chip with sensors cannot take precise point measurements, dipole contouring is necessary to:

- find the location of the zero line field in the axially symmetrical roller;
- locate polarity zones between different materials;
- determine the magnetomechanical effect;
- track the movement of the actuator rod;
- trace the magnetic field distribution at a required distance.

An isopleth is an equal value line, and dipole contouring consists in plotting magnetic isopleths similar to a weather map.

Presentation of the Maglab software package, either as autonomous or working with material testing machines, would extend far beyond the confines of this paper. Therefore, only a few selected applications of the software are presented below.

4.5. Application of the Magscanner-Maglab system to identify the Villari effect

Identification of an inverse magnetostriction (the Villari effect) for a plate with a circular hole (the so-called Kirsch specimen) subjected to cyclic loading is described in several papers [1, 5, 6, 15]. Such identification would make it possible to use a magnetic field image to describe the state of strain of a material and even the strain field in structural nodes made of ferromagnetic materials. However, there is a problem with a sufficiently precise local non-contact measurement of the magnetic field for different Kirsch specimen loading configurations. It should also be possible to generate a magnetic field image depending on the adopted magnetomechanical model of the Villari effect. Therefore, the Kirsch problem has been implemented in the Maglab software package whereby it becomes possible to determine the theoretical distribution of:

- a 2D state of stress;
- a 3D state of strain;
- specific energy;
- stress tensor axiator and deviator components.

The Maglab application can simulate the cyclic loading of the Kirsch specimen only in the elastic region for the selected geometry, which is signalled in the application. Using the elementary magnetomechanical models described in [6] and the Dipole Contouring Method one can obtain a 3D magnetic field distribution, also inside a hole, taking into account the edges of a sample. Figure 10 shows the Maglab windows used for defining the initial parameters and selecting the magnetomechanical model of the Kirsch specimen. In Fig. 10 no magnetic field strength H scale is given because the representation of H_x , H_y , H_z distributions around the hole for selected σ_{EF} models is of central importance.

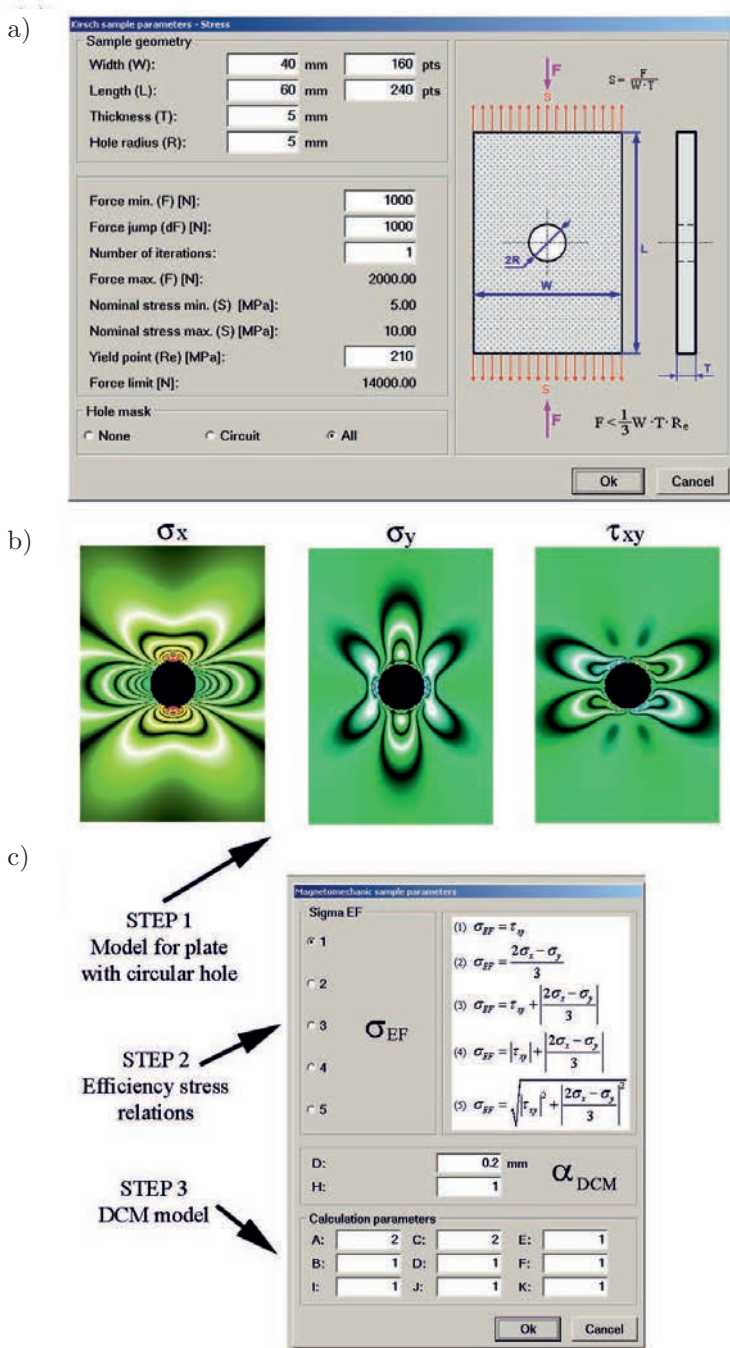


FIG. 10. Implemented DCM model for the plate with a circular hole (Kirsch specimen):
 a) the parameters of the sample geometry and loading selected to generate the stress distribution, b) the obtained stress distribution, c) selection of the magnetomechanical model [6, 16] and DCM parameters.

Figure 11 shows magnetic field distributions based on models 1, 2 and 5 [16].

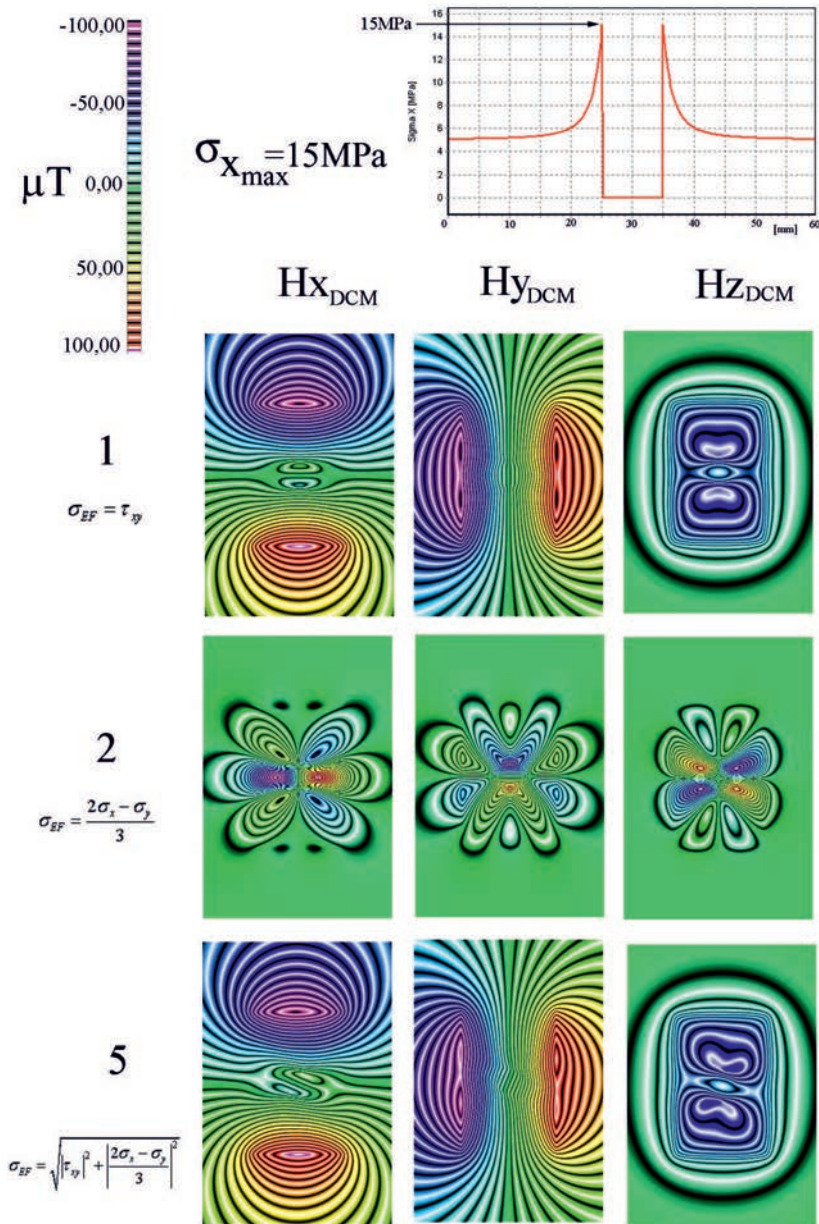


FIG. 11. Shapes of the magnetic field distributions around a circular hole in the loaded Kirsch specimen, computed in Maglab using the magnetomechanical models [16] and DCM.

The Magscanner-Maglab system uses a point-by-point scanning algorithm with simultaneous recording of the full loading period divided into a fixed num-

number of frames in order to determine the magnetic field distribution around a circular hole in a real Kirsch specimen subjected to cyclic loading.

Currently, the Magscanner-Maglab system can record periodic changes in the magnetic field around flat and cylindrical surfaces in the frequency range of 0.1–200 Hz at the resolution of 1/360. Thus, for repeatable conditions in the whole scanning range it is possible to produce maps of the magnetic field in a particular synchronizing signal phase. Cyclic loading of materials in the elastic range satisfies such requirements. Then the variable magnetic signal component is the Villari effect model.

Figure 12 schematically shows the point-by-point scanning algorithm and the generation of four maps, each with 360 frames or a prescribed number of frames. The current system can repeat point-by-point scanning after a break lasting a prescribed number of synchronization run periods. The box marked as ‘C’ (other sensor type) means that there is a possibility of using, for example, a photodiode.

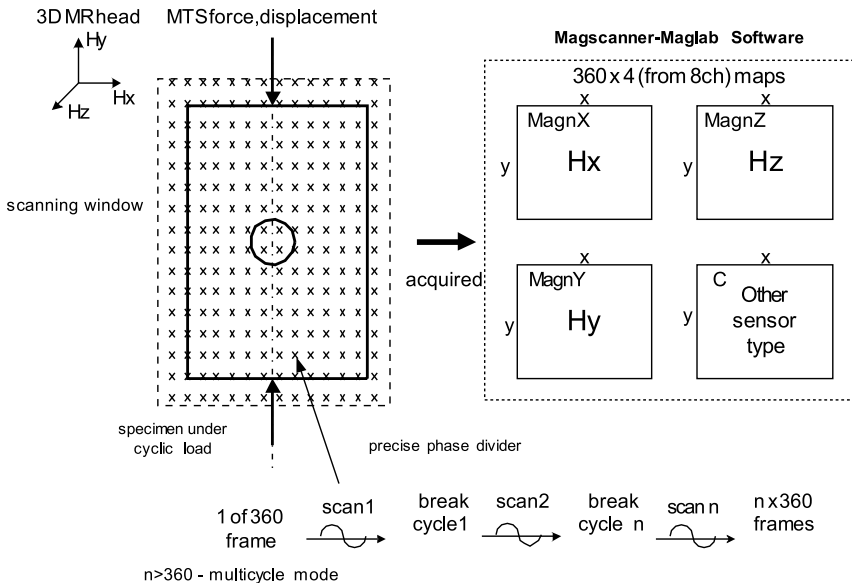


FIG. 12. Method of observing magnetic field vector aberration during a fatigue under a sinusoid loading.

Figure 13 shows the magnetic field distribution around a plate with a circular hole subjected to a symmetrical cyclic loading in three display modes: “RGB” – colours from the RGB palette are assigned to the magnetic field values, Isopleth – colours are separated by alternately black and white (creating the impression of contour lines on a map), and “AC” – the differential frame between the reference frame (reference phase of the signal) and all the recorded frames.

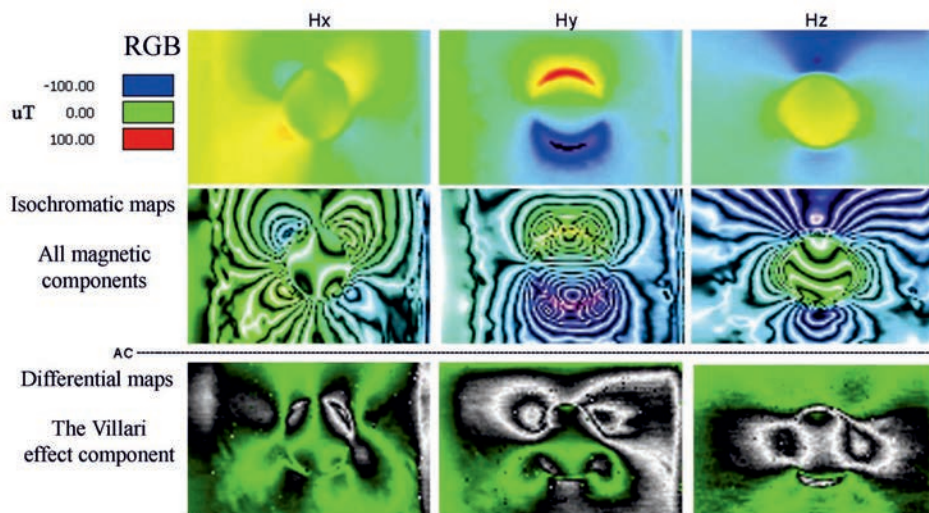


FIG. 13. Magnetic field distribution around a Kirsch specimen under a fatigue process, presented in three different modes of maps: RGB, isochromatic and differential isochromatic.

Consequently, a magnetic field distribution being solely the result of the Villari effect is obtained.

5. OTHER SELECTED APPLICATIONS

Exemplary applications of the scanner, featuring an earlier version of the magnetovision camera can be found in the papers [1, 4, 7–11, 14, 17] by the authors. New applications of the magnetovision system are connected with measuring the magnetic field around objects subjected to technological processing (cutting, laser ablation, electro-discharge drilling, micro-layer plotting, magnetic printing, etc.) in order to check their quality.

Figure 14 shows two such applications from the authors' independent experiments [18]. In the a) case it is the optical and magnetic image of the text which was laser engraved on steel. In the b) case the magnetic image of a letter 'A' sign on a disc is shown.

The Magscanner/Maglab (2010) system in its current version is a complete tool for magnetic investigations in mechanics. The system is capable of analyzing fatigue processes at low load frequency (up to 200 Hz) and registering the magnetic field vector in one degree steps (animated movie with 360 magnetic frames). Also, a handheld 3D digitizer for monitoring magnetic field strength has been designed, and its prototype has been built. The handheld wireless magnetoscanner incorporating a precision movement recorder is compatible with the Magscanner software and the other subsystems. The data acquisition unit is contained in the small Razer Lachesis computer mouse casing.

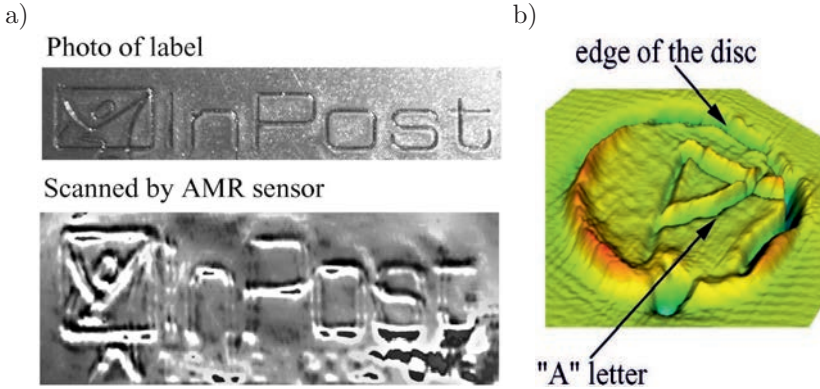
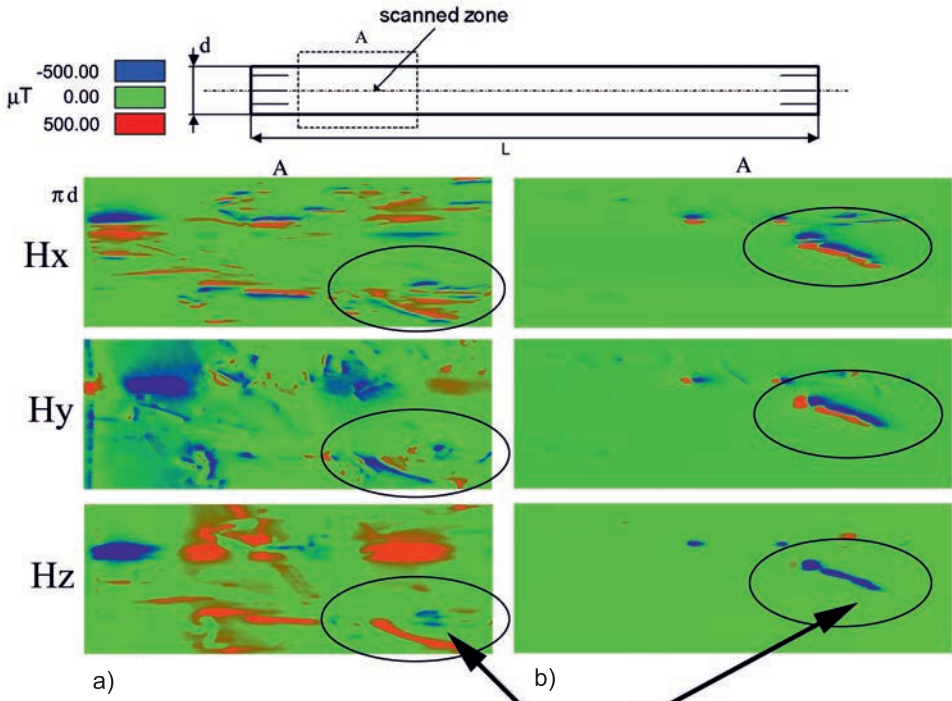


FIG. 14. Magnetic field strength disturbance used to detect changes on a ferromagnetic's surface: a) laser engraving, b) letter A sign on a disc [18].

The Magscanner/Maglab system can be used to control the quality of inductive hardening. Figure 15 shows magnetic field distributions on the cylindrical surface of a car axle shaft. The “Critical Zones” are specified as zones which run



Critical Zones as residual magnetic field distribution after induction hardening

FIG. 15. Rotational axis subsystem used for magnetic inspection of a car axle shaft: a) unhardened and b) after induction hardening.

the most risk of improper hardening, which shows itself in the larger range of magnetic field values close to the surface compared to the average distribution of the magnetic field on the shaft. Due to the use of the system a “Critical Zone” of the axle shaft can be controlled for improving the quality of inductive hardening.

6. CONCLUSIONS

1. A new generation of magnetic scanner for investigating various problems in experimental mechanics has been presented. The scanner enables the simultaneous determination of three magnetic field strength components H_x , H_y , H_z for flat and cylindrical objects. The non-contact measurement takes place at a set distance d from the investigated surface.
2. The measuring system is equipped with the Magscanner/Maglab software which enables signal acquisition, processing and visualization, also with the use of the Dipole Contour Method (DCM).
3. The possibilities of using the measuring system to identify the Villari effect model have been demonstrated for a plate with a circular hole subjected to cyclic loading.

Considering the above, it can be stated that the research objective has been achieved.

REFERENCES

1. J. KALETA, *Magnetomechanical Effect in Fatigue Investigations of Ferromagnetics*, Proc. of EUROMAT-2000, **2**, 1149–2254, 2000.
2. S. TUMANSKI, A. LISZKA, *Magnetic sensor array for investigations of magnetic field distribution*, J. Magn. Magn. Mat., **242–245**, 1253–1256, 2002.
3. C. H. SMITH, R. W. SCHNEIDER, M. TONDRA, *Biosensors: a New Use for Solid-State Magnetic Sensors*, Sensors Magazine, **16**, 12, 14–20, 1999.
4. J. KALETA, P. WIEWIÓRSKI, *Wireless 3D Magnetic Field Digitizer for inspection of parts fabricated using Smart Magnetic Materials*, Proc. of IV ECCOMAS Thematic Conference on Smart Structures and Materials, Porto, 2009.
5. J. KALETA, P. WIEWIÓRSKI, *Magnetovision as a Tool for Investigation of Fatigue Process of Ferromagnetics*; Proc. of Fatigue 2001, Sao-Paulo, December 12–14, 2001; 7, 2001.
6. J. KALETA, R. GÓRECKI, *Method of visualizing cross fields in plates subjected to cyclic loading. Fatigue and fracture mechanics* [in Polish], Proc. of XIX Symposium on Fatigue and Fracture Mechanics, Bydgoszcz, 2002.
7. J. KALETA, P. WIEWIÓRSKI, *Detection of defects in magnetic composite rods by means of high-resolution scanner* [in Polish], Acta Mechanica et Automatica, **1**, 1, 39–44, 2007.

8. J. KALETA, P. WIEWIÓRSKI, W. WIŚNIEWSKI, *Examination of texture of ferromagnetic sheets, using the Villari effect* [in Polish], Symposium on Mechanics of Failure of Materials and Structures, Augustów, 2003.
9. J. KALETA, P. WIEWIÓRSKI, W. WIŚNIEWSKI, *Magnetic memory of ferromagnetic material deformation history* [in Polish], Proc. of IX Domestic Conference on Fracture Mechanics, Kielce-Cedzyna, 14–17 September, 2003, Wydaw. P. Świętokrz., pp. 221–228, 2003.
10. B. FASSA, J. KALETA, P. WIEWIÓRSKI, *Methodology of investigating athermal martensite transformation in austenitic foils* [in Polish], Proc. of XIX Symposium on Fatigue and Fracture Mechanics, Bydgoszcz, 2002.
11. B. FASSA, J. KALETA, P. WIEWIÓRSKI, *Martensite transformation induced by plastic strain in foils made of metastable austenite* [in Polish], Proc. of VIII Domestic Conference on Fracture Mechanics, Kielce-Cedzyna, September 17–19, 2001; 8, Kielce, 2001.
12. S. TUMANSKI, S. BARANOWSKI, *Magnetic sensor array for investigations of magnetic field distribution*, J. Electr. Engin., **57**, 8/S, 185–188, 2006.
13. P. P. HORLEY, V. R. VIEIRA, P. D. SACRAMENTO, V. K. DUGAEV, *Application of the stereographic projection to studies of magnetization dynamics described by the Landau–Lifshitz–Gilbert equation*, J. Phys. A: Math. Theor., **42**, 315211 (11 p.), 2009.
14. J. KALETA, P. WIEWIÓRSKI, *The Dipole Contouring Method as a tool for magnetic field distribution in premagnetization zone in SMART actuator*, Proc. of IV ECCOMAS Thematic Conference on Smart Structures and Materials, 2009.
15. YANG EN, LI LUMING, CHEN XING, *Magnetic field aberration induced by cycle stress*, J. Magn. Magn. Mat., **312**, 72–776, 2007.
16. M. J. SABLİK, *Modelling the effects of biaxial stress on magnetic properties of steels with application to biaxial stress NDE, DPA*, Amsterdam, 1995.
17. J. KALETA, D. LEWANDOWSKI, P. WIEWIÓRSKI, *3D magnetovision scanner as a tool for investigation of magnetomechanical principles*, Solid State Phenomena, **154**, 181–186, 2009.
18. J. KALETA, P. WIEWIÓRSKI, *Construction of magnetic scanner for application in experimental mechanics*, Proc. of 26th Danubia-Adria Symposium on Advances in Experimental Mechanics, pp. 95–96, Leoben, September 23–26, 2009.